DEVELOPMENT, OPTIMIZATION, AND *IN-SILICO* STUDIES OF HESPERIDIN-SOYA PHOSPHATIDYLCHOLINE COMPLEX

Debarshi Kar Mahapatra[1], Richa Tripathy[1], Shailendra Patil[2], Asmita Gajbhiye Patil[1]*

Abstract

Natural products lack their charm due to several factors like absorption, first-pass metabolism, rapid biotransformation, efflux transport mechanisms, food effects, or numerous other factors which leads to low therapeutic efficacy and frequently impose a question mark over their acceptance. To resolve this issue, using the formulation optimizer Design Expert® software v.12.0, the optimal ratio of hesperidin (flavonoid)-soya Phosphatidylcholine (SPC) was calculated using factorial arithmetic, with three critical factors (complexation rate, entrapment efficacy, and drug release) considered. From the above statistical treatment, hesperidin-SPC in the optimized ratio of 1:1 was developed through conventional method. The developed product was comprehensively characterized through spectroscopic techniques (through Ultraviolet-Visible, Fourier-transformed Infrared, and Nuclear Magnetic Resonance; thermal studies (through Differential Scanning Calorimetry and Thermal Gravimetric Analysis), Crystallinity (through X-ray diffraction), morphology (through Compound Microscopy, Scanning Electron Microscopy and Atomic Force Microscopy), and Composition (Energy-dispersive X-ray spectroscopy). In addition to it, the complex was broadly studied through *in-silico* parameters in terms of chemistry, physicochemical, pharmacokinetics, metabolism, toxicity, and biology using the computational tool Swiss ADME. In conclusion, the critical elements were researched *in silico*, the best optimal ratio was established, the essential components were explored, and the negative effects of different factors were mitigated, allowing for the development of the phytosomes.

Keywords: Hesperidin, Flavonoid-SPC Complex, Design Expert, Optimization, *In silico*, Phytosomes

[1*]Department of Pharmaceutical Sciences, Dr. Hari Singh Gour Vishwavidyalaya (A Central University), Sagar 470003, Madhya Pradesh, India
[2]Department of Pharmaceutics, SVN Institute of Pharmaceutical Sciences, Swami Vivekanand University, Sagar 470228, Madhya Pradesh, India

***Corresponding Author:** Asmita Gajbhiye Patil
*Department of Pharmaceutical Sciences, Dr. Hari Singh Gour Vishwavidyalaya (A Central University), Sagar 470003, Madhya Pradesh, India, E-mail: asmitapatil27@rediffmail.com

DOI: 10.48047/ecb/2023.12.si10.0013

1. Introduction

With the fast changing trends in modern pharmacotherapeutics, natural products are playing an imperative role. The shift and believe among the masses of preferring herbal based medicines in present day market has revolutionized the traditional medicines and also opened avenues for phytotherapy [1]. The phytoconstituents of varied classes constitute the main active moiety for modulating several biochemical pathways in the human body associated with the physiological processes and disease progression like cancer, diabetes, inflammation, etc. It has been estimated that nearly 74% of the modern-day drug are having structural resemblance with the products of natural origin where either they are suitably modified through semisynthetic approaches or through inspiration from the reported scaffolds of the compounds to obtain pronounced activity [2].

As the sophisticated drug discovery processes revolutionized in this decade, several *in silico* and *in vitro* screening have revealed the pharmacological potentials of numerous natural products. Similarly, when *in vivo* studies were performed all of them expressed biological activity to varied magnitude but with "compromised pharmacokinetic profile". The years-long tedious process of drug discovery and development which involve identification cum optimization of a single 'lead' from trillions of candidates, perhaps face the harsh ending of 'rejection from clinical trial Phase-I' [3]. In the last decade, the whole researcher community has witnessed that nearly 93% of the drugs of Alzheimer's disease, carcinoma, hepatitis, etc. failed to cross the Phase-I of the clinical trials. The most common reason observed in all the cases is 'failure in bioavailability and pharmacokinetic profile' where the lead molecule demonstrated either too long or too short t½, poor absorption, or extensive first-pass metabolism [4].

Flavonoids consist of a large group of polyphenolic compounds having a benzo-β-pyrone structure and are ubiquitously present in plants. They are synthesized by phenylpropanoid pathway and are considered as "nature's biological response modifiers". Flavonoids exhibit multifarious pharmacological activities like hypoglycemic, anti-proliferative, antioxidant, antihypertensive, anti-platelet, anti-arrhythmic, anti-obesity, anti-malarial, anti-tubercular, antifilarial, anti-retroviral, anti-protozoal, anti-fungal, anti-bacterial, sedative, anxiolytic, anti- Alzheimer's disease, anti-nociceptive, anti-inflammatory, anti-ureate, osteogenic, anti-invasive, and anti-allergic [5-6]. Some well-known flavonoids such as hesperidin, quercetin, mangiferin, kaempferol, myricetin, rutin, genistein, luteolin, etc. play a key role in pharmacotherapy [7].

However, these experimentally proven pharmacodynamics results also presented strikingly poor pharmacokinetics and hence, reasonably reduced bioavailability. The serum concentration for the flavonoids; quercetin (14 μmol/L), rutin (65 μmol/L), mangiferin (92 μmol/L), kaempferol (76 μmol/L) indicates a much compromised pharmacokinetic profile and hence bioavailability in the range of 17 to 37% [8-9]. Many herbal formulations containing flavonoids or single-ingredient phytoconstituent(s) like hesperidin capsule (Brand: Aller-Sine®) lack their charm due to several factors like absorption, first-pass metabolism, rapid biotransformation, efflux transport mechanisms, food effects, or numerous other factors which leads to low therapeutic efficacy and frequently impose a question mark over their acceptance [10].

The present study highlights an attempt to overcome pharmacodynamics characteristics and pharmacokinetic attributes of a well-known flavonoid (Hesperidin) via development of lipid complexes (Soya phosphatidylcholine). Using the formulation optimizer Design Expert® software v.12.0, the optimal ratio of hesperidin (flavonoid)-soya Phosphatidylcholine (SPC) was calculated using factorial arithmetic ($x - A + B - AB - A^2 - B^2$), with three critical factors (complexation rate, entrapment efficacy, and drug release) considered. The study includes comprehensive characterization of product through spectroscopic techniques (through Ultraviolet-Visible, Fourier-transformed Infrared, and Nuclear Magnetic Resonance; thermal studies (through Differential Scanning Calorimetry and Thermal Gravimetric Analysis), Crystallinity (through X-ray diffraction), morphology (through Compound Microscopy, Scanning Electron Microscopy and Atomic Force Microscopy), and Composition (Energy-dispersive X-ray spectroscopy). In addition to it, the complex was broadly studied through *in-silico* parameters in terms of chemistry, physicochemical, pharmacokinetics, metabolism, toxicity, and biology using the computational tool SwissADME.

2. Materials and Methods

2.1. Materials

Hesperidin was obtained as procured from Sigma Aldrich Ltd., Mumbai, India. Soya phosphatidylcholine (SPC) was obtained from Hi-Media Ltd., Mumbai, India. All other reagents and solvents were of analytical grade and obtained from

SD Fine Chemicals Ltd., Mumbai, India. Distilled water was used throughout the study.

2.2. Optimization of ratio

The drug entrapment effectiveness stays extremely low as a drug complex forms, according to the literature. In order to overcome this problem, different drug and lipid concentrations were investigated to see how they affected drug release, entrapment effectiveness, and complexation rate. For products, a two-factor, three-level factorial design (3^2) was used with medication (X_1) and lipid (X_2) concentrations chosen as independent variables. Experimental batches were run at each variable's three levels in all nine potential combinations. The other variables remained unchanged. The analysis of the data was done to see how independent factors affected dependent variables. By constructing a polynomial equation with a regression coefficient, Design Expert was used to do multiple regression analysis (MRA), analysis of variance (ANOVA), and statistical optimisation. A positive sign denotes a positive effect on the response, and a negative sign denotes a negative effect on the answer, indicating the influence of a specific phrase on the response [11].

2.3. Formation of hesperidin-SPC complex

Hesperidin (0.002 M; 1.22 g) and soya phosphatidylcholine (0.002 M; 1.516 g) were made to react in dichloromethane solvent under reflux condition at 50 rpm stirring, until a clear solution was formed. The above content was diluted with 50 mL of n-hexane and shakened in a separating funnel. The above content was allowed to stand overnight for the precipitation of the hesperidin-SPC complex. The complex was filtered by Whatman Filter Paper and further thoroughly washed with n-hexane for 3 times to remove the adhered SPC. The amorphous complex was dried and stored at 4°C [12] (**Figure 1**).

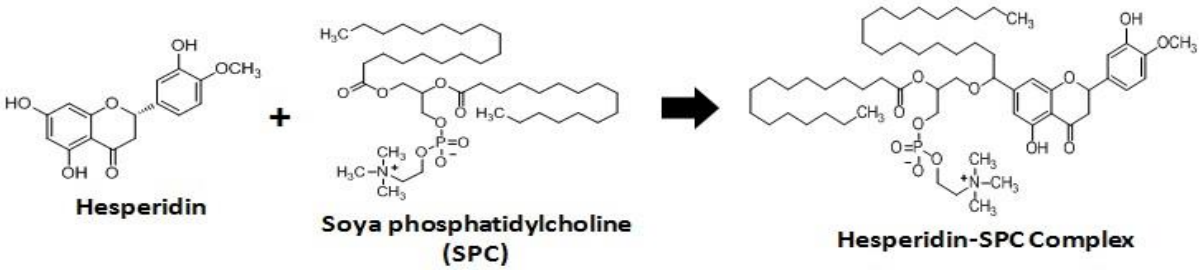

Figure 1. Development of hesperidin-SPC complex.

2.4. Characterization of hesperidin-SPC Complex

2.4.1. Complexation efficiency study

The drug entrapped in the complex was determined by taking the dialyzed vesicular suspension (1 mL in quantity) and further digesting the content with Triton X-100 (0.1 mL) for the duration of 5 min. The produced solution was centrifuged at 3000 rpm for the duration of 5 min and the supernatant was decanted off. The above content was properly diluted with methanol and analyzed spectrophotometrically (Shimadzu® UV-1800, Kyoto, Japan) at 272 nm, using Triton X-100 as a blank. The complexation efficiency was determined using the formula [13]:

Complexation rate (%) = $(m_2/m_1) + [(m_1–m_3)/m_1] \times 100$

Where, m_1 is the total content of hesperidin added, m_2 is the content of hesperidin present as a complex and m_3 is free hesperidin

2.4.2. Solubility studies

The solubility profile of the hesperidin, SPC, and hesperidin-SPC Complex was studied by taking 2 mg of the substance in different solvents (distilled water, chloroform, methanol, dichloromethane, and n-hexane) of 10 mL volume in the small volumetric flasks [14].

2.5. Instrumental analysis of Hesperidin-SPC Complex

2.5.1. Ultraviolet-Visible Spectroscopy

The formation of hesperidin-SPC complex from hesperidin was investigated using UV-Vis Spectrophotometer (Shimadzu UV-1800, Kyoto, Japan) in the wavelength range of 200–800 nm. Small sample aliquots of the colloids were prepared with double distilled water and recorded [15].

2.5.2. Fourier-transformed Infrared Spectroscopy

FTIR absorption spectrum of hesperidin and hesperidin-SPC were recorded by potassium bromide dispersion technique in the range of 4000–400 cm−1 in FTIR spectrophotometer (Shimadzu® IRAffinity-1, Kyoto, Japan). The samples were scanned at a resolution of 0.15 cm^{-1} and scan speed was 20 scan/s [16].

2.5.3. X-ray diffraction

X-ray diffraction study describes an effective way to procure information on the crystallinity and shape of PXRD patterns reveals the arrangement of molecules in the crystals. The solid-state characterizations of hesperidin and hesperidin-SPC complex were performed by X-ray powder scattering measurements using X-ray diffractometer (Shimadzu IRAffinity-1, Kyoto, Japan). The measurements were performed at room temperature using monochromatic CuK- radiation at 40 kV over a 2 theta range of 4–40° with a continuous scanning speed of 4° min^{-1} [17].

2.5.4. Differential Scanning Calorimetry

Thermal transition properties of hesperidin and hesperidin-SPC complex were measured on differential scanning calorimeter (Mettler Toledo®, UK). Sample powder was weighted and sealed in an aluminum DSC pan. After holding isothermally at 30°C for 1 min, DSC scanning was performed from 30°C to 300°C at a heating rate of 10°C min^{-1} under a dry nitrogen purge of 50 mL min^{-1}. An empty pan served as reference [18].

2.5.5. Microscopy

2.5.5.1. Simple Microscopy

The morphological characteristics of hesperidin and hesperidin-SPC complex were thoroughly studied under a compound microscope under a magnification of 40X. The microphotographs were recorded using a mobile camera [19].

2.5.5.2. Scanning Electron Microscopy

The external morphological characteristics of the hesperidin-SPC complex were studied by scanning electron microscopy. The lightly sprinkled samples were gold coated by mounted on aluminum stub (3–5 nm; 75 s; 40 W) to make them electrically conductive. Micrographic images were taken at a different magnification with an acceleration voltage of 10 kV [20].

2.5.5.3. Atomic Force Microscopy

Hesperidin-SPC was imaged with an atomic force microscope (Molecular Imaging, USA) operating in the acoustic ac mode, with the aid of a cantilever (NSC, MikroMasch) [21].

2.6. Computational studies

2.6.1. Pharmacokinetics, Bioavailability, and Drug-likeliness studies

A pharmacokinetics prediction research was conducted, looking at ADME, bioavailability, and ligand drug-likeness using the SwissADME online tool. Bioavailability radar is computed using the following six physicochemical parameters to identify drug-likeness: lipophilicity, size, polarity, insolubility, flexibility, and insaturation. Passive human gastrointestinal absorption (HIA), blood-brain barrier (BBB) penetration, and permeability glycoprotein (P-gp) substrate/non-substrate status were all found to be positive or negative in the tool's internal BOILED-Egg model. WLOGP is an implementation of a purely atomistic method, XLOGP3 is an atomistic method with corrective factors and a knowledge-based library, and MLOGP is an archetype of topological method relying on free energies of solvation in n-octanol and water calculated by the generalized-born and solvent accessible surface area (GB/SA) model. The Lipinski (Pfizer) filter was the first rule of five to be put into a tool for predicting drug-likeness. Oral bioavailability was predicted using the bioavailability radar, which takes into account a wide range of physicochemical parameters [22].

2.6.2. Drug Target Identifications

An online tool for predicting the targets of bioactive molecules known as Swiss Target Prediction makes it possible to foresee the targets. A combination of 2D and 3D similarity measures are used to compare the query molecule to a library of 280,000 compounds active on more than 2000 targets in five different species. Mapping the targets of bioactive small molecules is necessary for comprehending the molecular mechanisms behind bioactivity and for anticipating any adverse effects or cross-reactivity. Predictions have been produced in three different organisms (models), and mapping predictions by homology within and between species is doable for close paralogs and orthologs. It has been demonstrated that the rat (*Rattus norvegicus*), mouse (*Mus musculus*), and human (*Homo sapiens*) models all have reliable inhibitory targets for the hesperidin-SPC complex [22].

3. Results and Discussion

3.1. Statistical optimization of ratio

In the optimization study, it was found that the most optimized ratio of drug to phospholipid for all the three cases was 1:1 **(Figure 1)**. The individual equations derived for complexation rate, particle size, and entrapment efficacy along with other information (such as desirability = 1.0) for all the hesperidin is given below:

Complexation Rate = +71.32 +1.52 A -1.20 B -18.83 AB

Entrapment Efficacy = +69.79 +1.75 A -2.64 B -10.40 AB

Drug Release = +81.82 - 0.4050 A +1.77 B -14.03 AB +8.73 A^2 -10.34 B^2

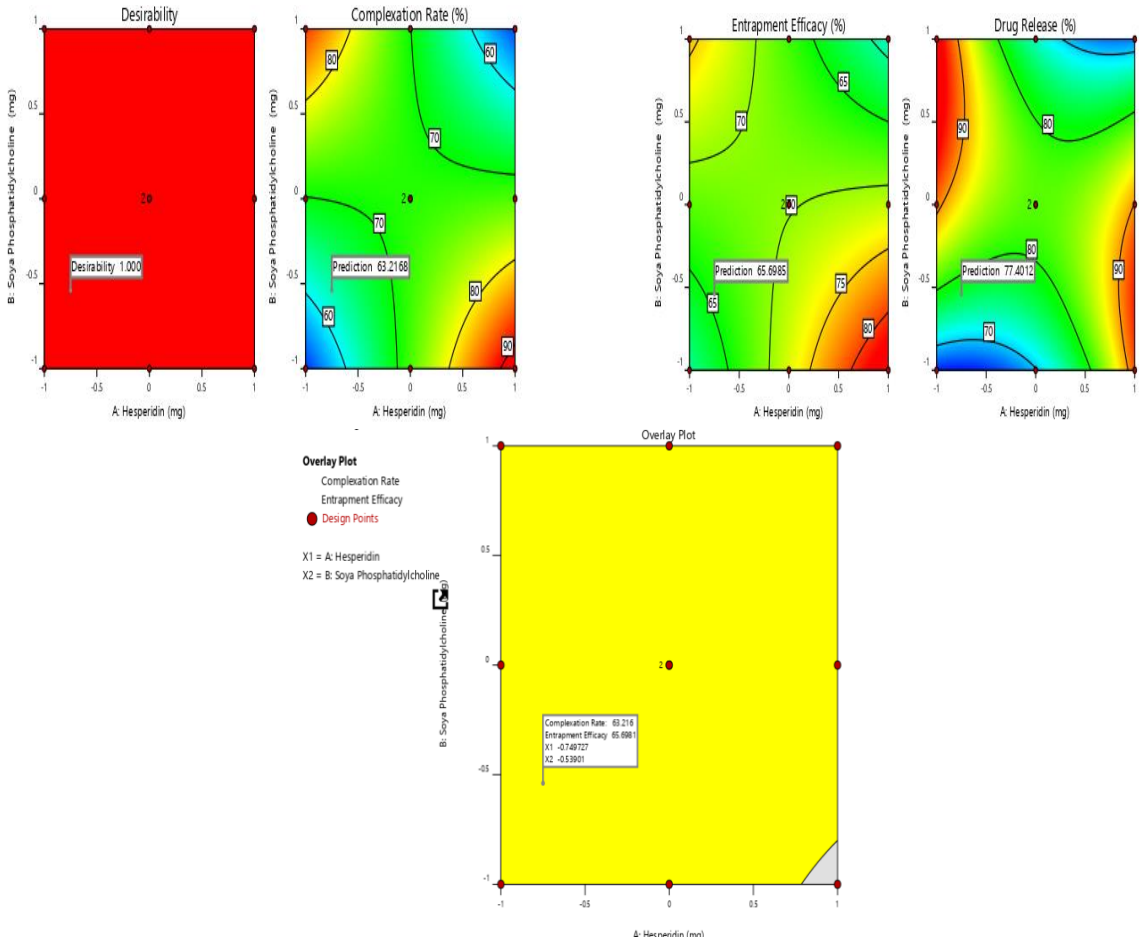

Figure 1. Response surface plot, overlay plot, and counter plot illustrating the influence of drug-lipid complex on complexation rate, particle size, and entrapment efficacy.

3.2. Characterization of hesperidin-SPC Complex

3.2.1. Complexation rate

The complexation rate was found to be sufficiently high (87.67%) indicating sufficiently high complex formation of hesperidin with SPC.

3.2.2. Solubility studies

The parent molecule (Hesperidin) demonstrated slightly soluble characteristics in distilled water and in *n*-hexane. In contrast to it, the complex (hesperidin-SPC) showed formation of micellar solution which is indicative of the fact that the complex attains better solubilization characteristics or the molecule. Alike, a good solubility was observed for the complex in *n*-hexane. The solubility characteristics of both drug and lipid-complex for the solvents; dichloromethane and chloroform were found to be similar demonstrating soluble characteristics **(Table 1)**.

Table 1. Solubility profile of hesperidin and hesperidin-SPC.

Solvent	Hesperidin	SPC	Hesperidin-SPC
Distilled water	Slightly soluble	Form micellar solution	Form micellar solution
Methanol	Sparingly soluble	Soluble	Soluble
Dichloromethane	Soluble	Soluble	Soluble
Chloroform	Soluble	Soluble	Freely Soluble
n-hexane	Slightly soluble	Sparingly soluble	Soluble

3.3. Instrumental analysis of hesperidin-SPC Complex

3.3.1. Ultraviolet-Visible Spectroscopy

The corresponding absorption maxima (λmax) were perceived at 272 nm and 349 nm for hesperidin (**Figure 2A**). It was evidenced from the literature that some flavonoids have multiple λmax values, which hold true in this case for hesperidin and catechin which showed two λmax values. After the complexation, a change in the absorption maxima was observed which ascertained the formation. In the case of hesperidin-SPC complex, the λmax shifted to 276 nm and 379 nm (**Figure 2B**).

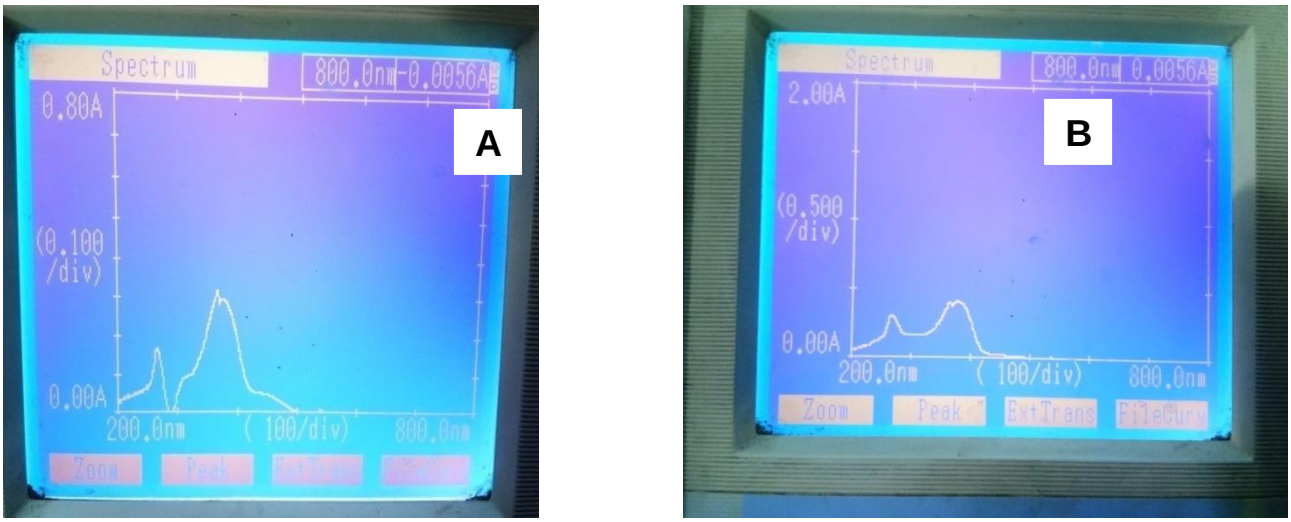

Figure 2. UV-Vis spectra: (A) Hesperidin (B) Hesperidin-SPC Complex.

3.3.2. FT-IR Spectroscopy

The pure flavonoid hesperidin expressed characteristic hydroxyl peaks (cm^{-1}) at 2921.69 and 2851.38 along with other characteristics peaks (cm^{-1}) at 1740.62, 1641.12, 1518.91, 1180.59, 1047.49, 974.05, 844.28, 816.25, 765.88, and 737.36 (**Figure 3A**). The FTIR spectra of the fabricated complexes showed disappearance of characteristic peaks of hydroxyl group in the range 2850 cm^{-1} to 3000 cm^{-1} [2921.69 cm^{-1} and 2851.38 cm^{-1}] which supported the reaction of phenolic –OH (at third-position) group of flavonoids at choline part of SPC that confirms the formation of complex (**Figure 3B**).

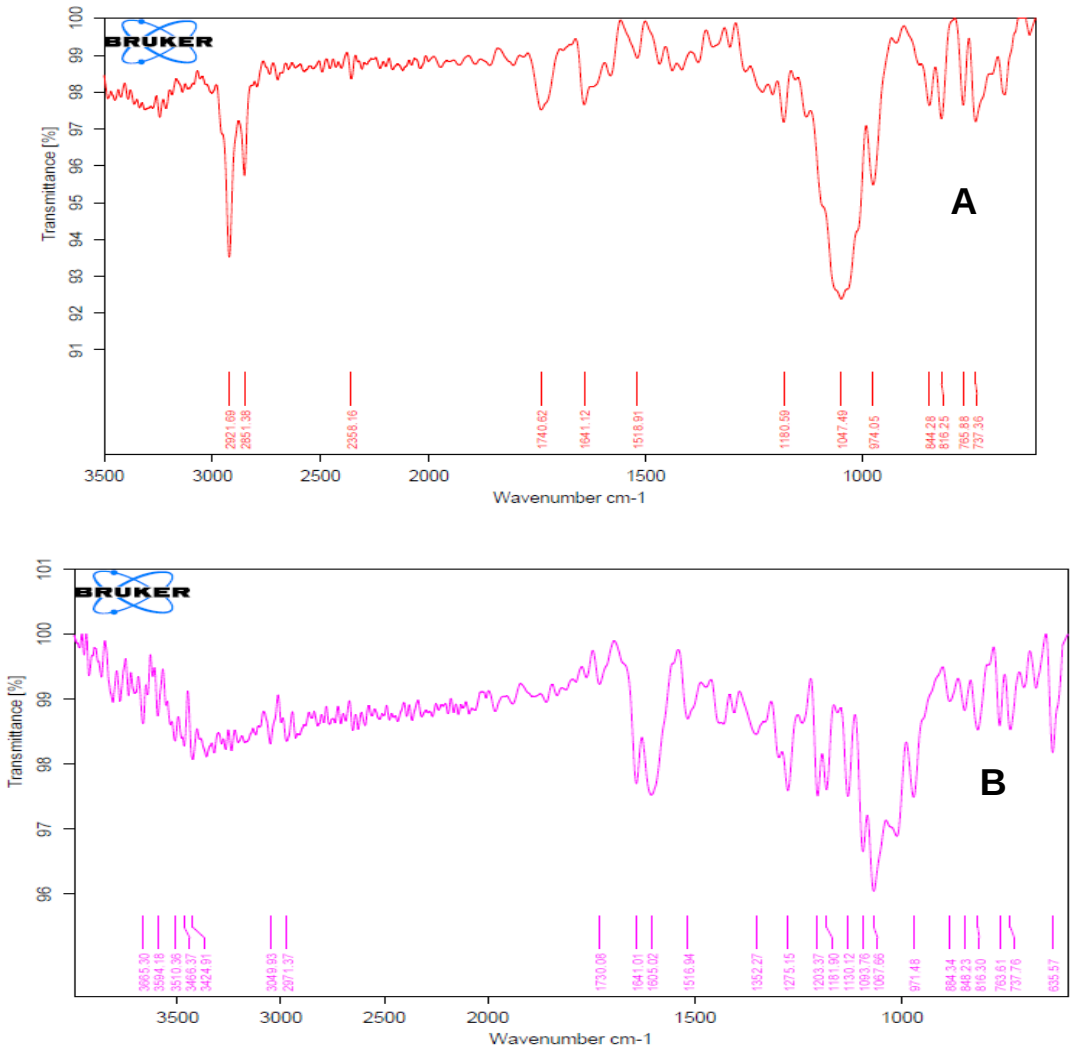

Figure 3. FTIR spectra: (A) Hesperidin (B) Hesperidin-SPC Complex.

3.3.3. X-Ray Diffraction study

The appearance of several intense crystalline peaks reflects the existence of pure flavonoid in crystalline state. Hesperdin showed characteristic peaks (2θ) at 12.043(19), 13.56(4), 15.441(13), 16.102(11), 18.47(4), 19.459(9), 21.180(15), 22.287(11), 23.73(3), 24.69(3), 27.63(8), 28.578(19), 31.88(5), 32.82(7), 34.66(3), 37.15(2), and 43.93(13) (**Figure 4A**). However, an analysis of PXRD pattern of the complex depicted no such significant peaks which stalwartly confirmed the molecularly complexed state of flavonoid in the formulation and effective solubilization (**Figure 4B**). The drug experienced swift renovation from crystalline state to its amorphous form, which is having high internal energy, thereby resulting in prompt dissolution of drug materials as compared to its crystalline forms.

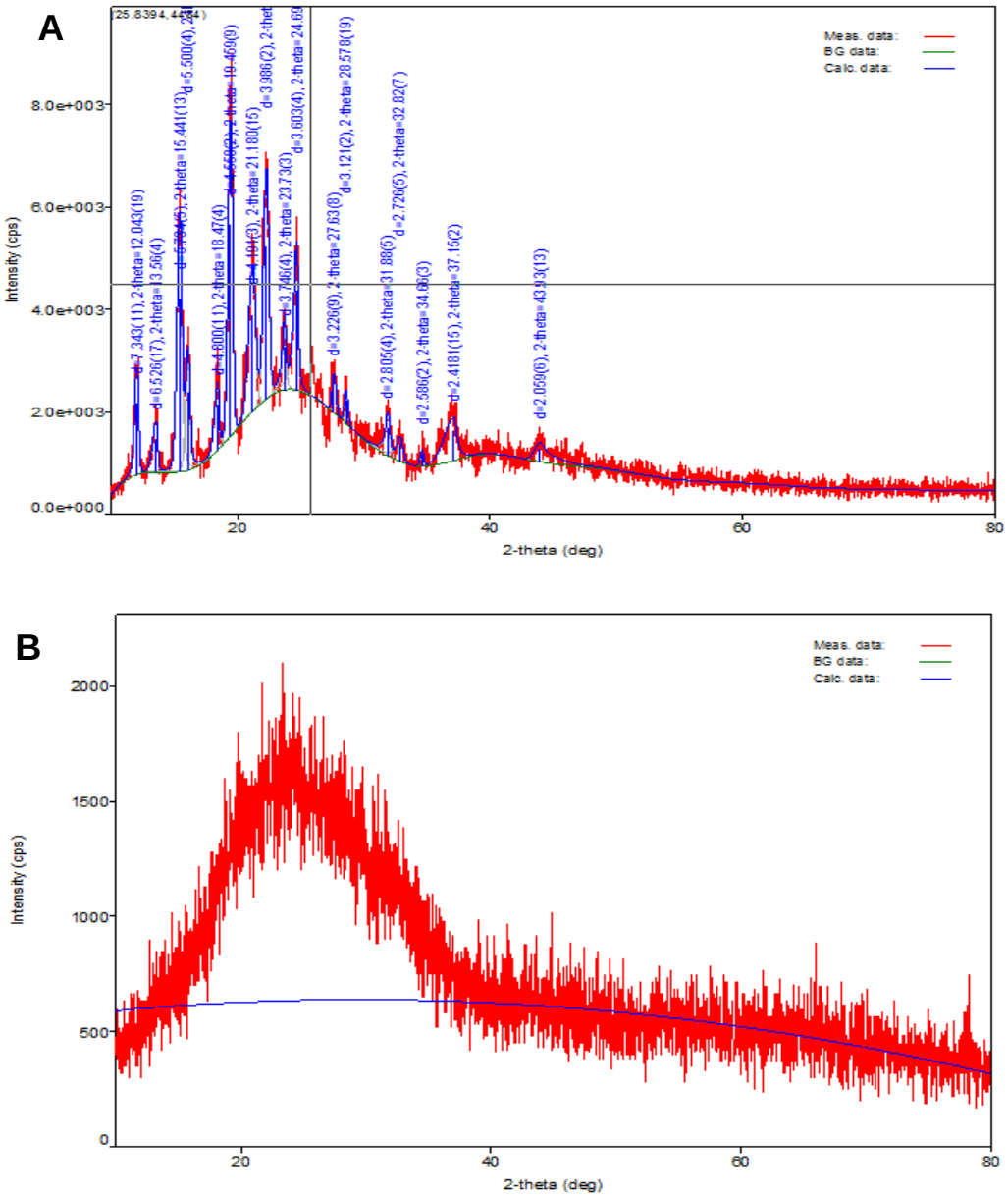

Figure 4. X-ray diffractogram: (A) Hesperidin (B) Hesperidin-SPC Complex.

3.3.4. Differential Scanning Calorimetry

The flavonoid expressed characteristic endothermic onset peak corresponding to the melting point of hesperidin; *i.e.* 256.14°C (**Figure 5**). The thermogram of the SPC complex demonstrated a broad endothermic peak for hesperidin at 107.91°C, over the entire scanning range of 30°C-300°C, suggesting the formation of the complex into a single entity and their rapid transformation into amorphous nature. Thus, it may be concluded that no such characteristic pure flavonoid peak indicated the change in melting behavior of flavonoid and inhibition of crystallization since amorphous state is considered as a state of high disorder, the solid particles present remain in highly complexed state that eventually promoted rapid aqueous solubility.

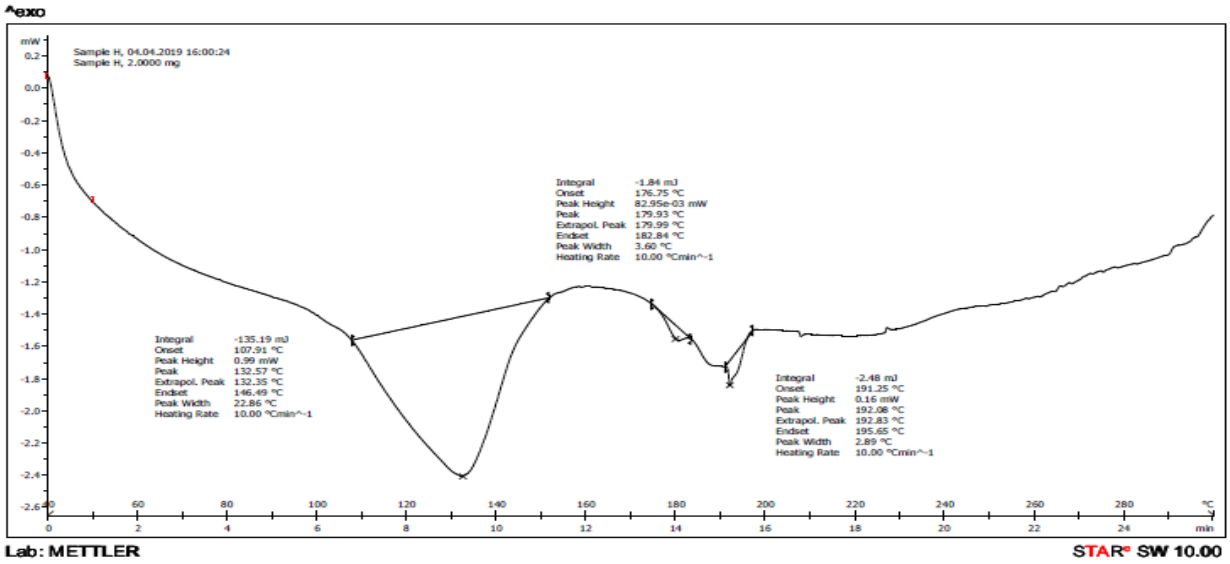

Figure 5. DSC thermogram of hesperidin-SPC complex.

3.3.5. Microscopy

3.3.5.1. Simple Microscopy

The simple microscopy revealed that hesperidin was coarse, exists in agglomerates, and clumps **(Figure 6A)**. However, the formed product (hesperidin-SPC) was found to be quite small, exists in separate entities, and has thread-like morphology **(Figure 6B)**.

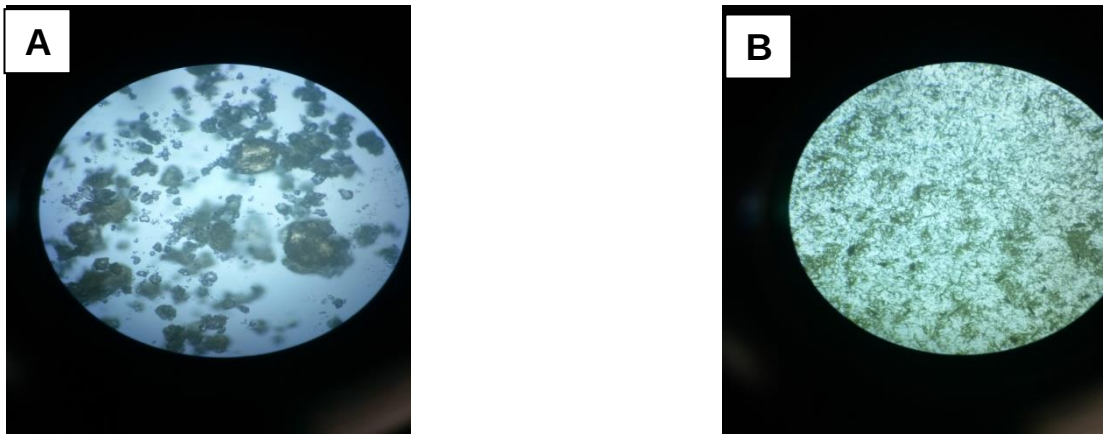

Figure 6. Visual observation: (A) Hesperidin (B) Hesperidin-SPC Complex.

3.3.5.2. Scanning Electron Microscopy

The microphotographs (500x magnification) showed uniform surfaces, nearly-smooth particle with aggregated irregular particles and deep crevices. This suggested that entire drug was distributed uniformly in the complexes as amorphous components in micro size (50-75 µm range) (**Figure 7**).

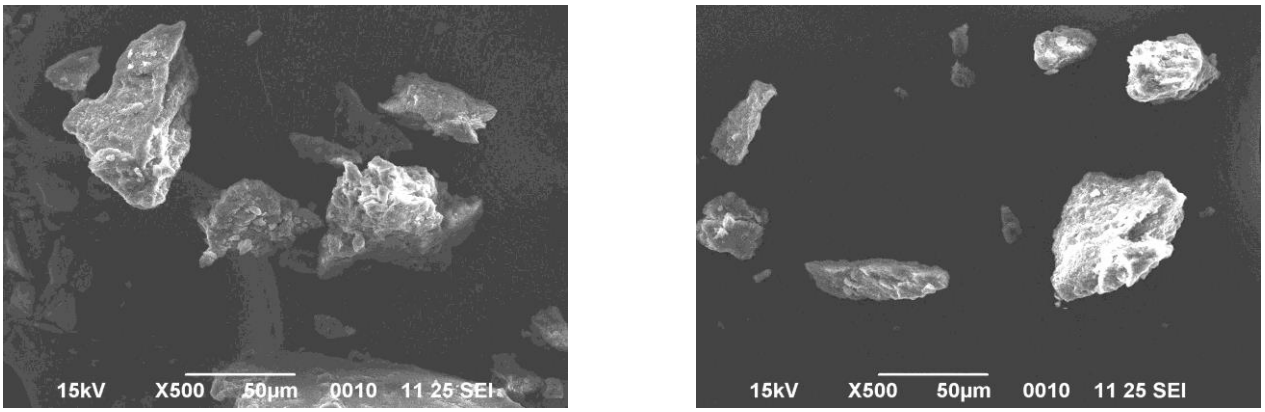

Figure 7. Photomicrographs of hesperidin-SPC complex at 500x magnifications.

3.3.5.3. EDAX analysis

The EDAX analysis of hesperidin-SPC complex demonstrated the presence of multiple elements. Carbon was found to be in highest abundance (65%) whereas silicon (<1%) was present in lowest abundance (**Figure 8**). Other elements such as oxygen (>5%), phosphorous (>1%), and potassium (20%) were also present in the complex.

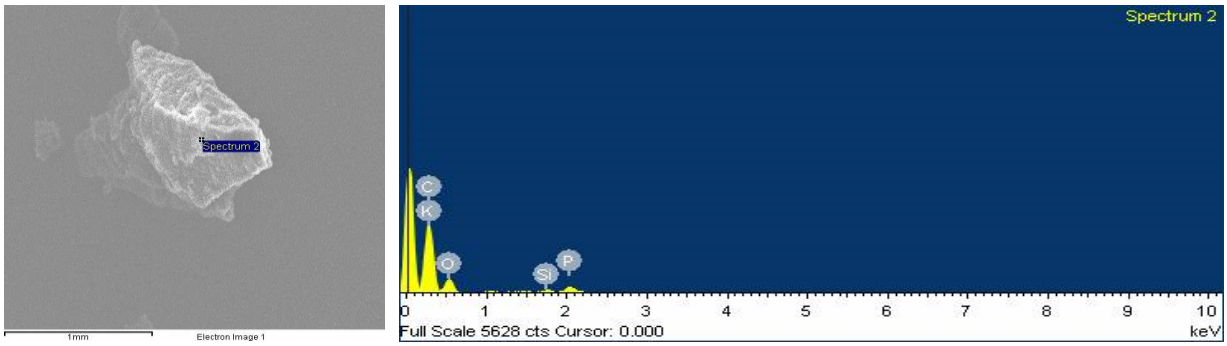

Figure 8. EDAX analysis of hesperidin-SPC complex.

3.3.5.4. Atomic Force Microscopy

Multiple micro-sized round shaped components were seen that eventually confirmed the formation of the complex and derived certain imperative facts: amphiphilic characteristics, non-surfactant nature, uniform surface height, smooth external surface, and irregular morphology (**Figure 9**). The formation of SPC complex with hesperidin was ascertained from AFM study.

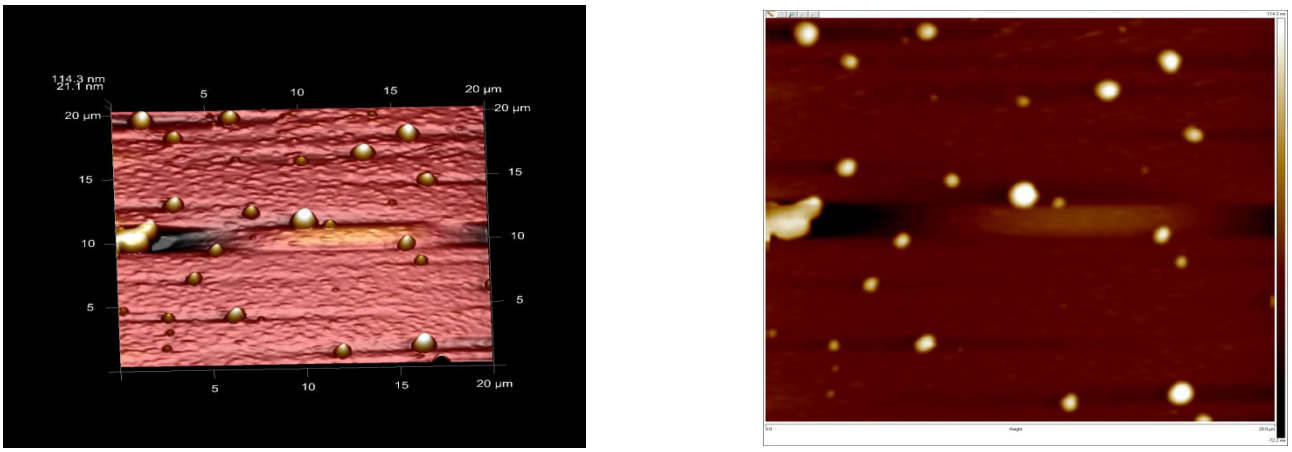

Figure 9. Atomic Force Microscopy of hesperidin-SPC complex.

3.5. Computational studies

3.5.1. Pharmacokinetics, Bioavailability, and Drug-likeliness studies

Table 2 describes the predictive values for pharmacokinetics, bioavailability and drug-likeness data on hesperidin-SPC Complex. The molecule showed high absorption rate. Low blood-brain permeability was obtained based on Log P value while higher negative value indicated lower skin permeation. In case of metabolism, the molecule did not prove to be a p-glycoprotein substrate as well as for CYP1A2, CYP2C19, CYP2C9, and CYP2D6 inhibitors, except for CYP3A4. For the prediction of bioavailability and drug-likeness, an optimal bioavailability score was obtained. Low water solubility was obtained for hesperidin-SPC Complex. The bioavailability radar for oral bioavailability prediction showed desired INSATU = insaturation as per Csp3 as 0.76, FLEX as per number of rotable bond 45, POLAR as TPSA (Å²) 179.92, and LIPO as XLOGP3 value of 17.33 (**Figure 10A**).

In case of BOILED-Egg model (**Figure 10B**), it was obtained that hesperidin-SPC Complex has no capability of blood-brain barrier penetration as well as it also showed high penetration power of gastrointestinal absorption. The molecule was found to be PGP neutral substrate in predictive model. Interestingly, the Brain Or IntestinaL Estimate D permeation method (BOILED-Egg) has already been proposed as an accurate predictive model, which helps by computational prediction of the lipophilicity and polarity of small molecules. In overall predictive results, hesperidin-SPC Complex can be suitable drug candidate as per bioavailability radar and BOILED-Egg representation.

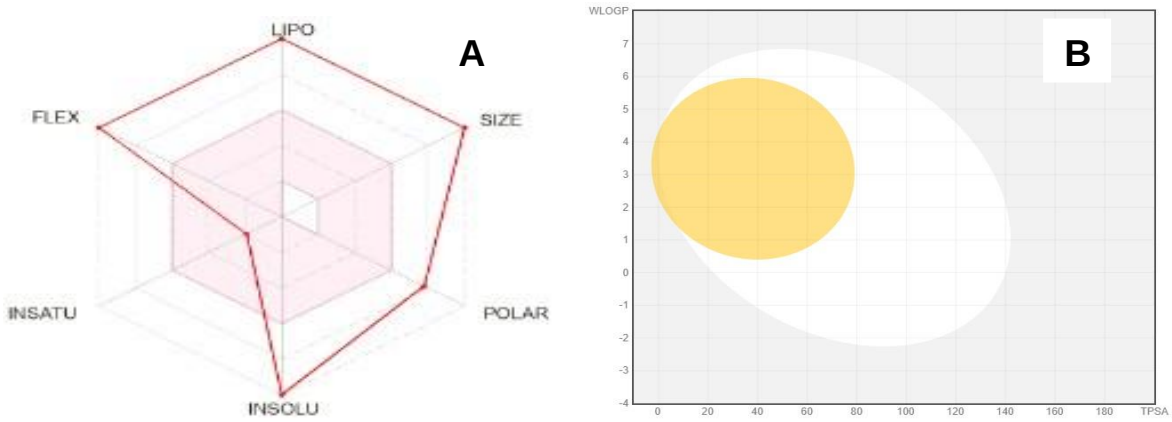

Figure 10. Pharmacokinetic predictions for hesperidin-SPC complex: (A) Bioavailability radar plot and (B) BOILED Egg Model.

Table 2. Pharmacokinetics and physicochemical properties of hesperidin-SPC complex.

Pharmacokinetics		
GIT absorption	High	Good oral absorption
BBB permeant	No	Cannot penetrate BBB
P-gp substrate	No	Cannot efflux molecule
CYP1A2 inhibitor	No	No metabolism
CYP2C19 inhibitor	No	No metabolism
CYP2C9 inhibitor	No	No metabolism
CYP2D6 inhibitor	No	No metabolism
CYP3A4 inhibitor	Yes	Highly metabolized
Log Kp (skin permeation)	-0.29 cm/s	No skin penetration
Log Po/w (iLOGP)	7.33	Highly lipophiliic
Log Po/w (XLOGP3)	17.33	Highly lipophiliic
Log Po/w (WLOGP)	15.16	Highly lipophiliic
Log Po/w (MLOGP)	1.02	Highly lipophiliic
Log Po/w (SILICOS-IT)	13.12	Highly lipophiliic
Consensus Log Po/w	10.79	Highly lipophiliic
Bioavailability Score	0.55	Good Bioavailability after oral administration
Physicochemical Properties		
Number of heavy atoms	72	-
Number of aromatic heavy atoms	12	-
Fraction Csp3	0.76	-
Number of rotatable bonds	45	-
Number of H-bond acceptors	12	-
Number of H-bond donors	2	-
Molar Refractivity	223.30	-
TPSA	179.92 A^2	-
Synthetic accessibility	9.94	-
Solubility	5.03e-12 mg/ml	Low solubility

3.5.2. Drug Target Identifications

As the study is focused on drug repurposing, it remains crucial to determine the plausible therapeutic targets against which Hesperidin–SPC complex can inhibit them with micromolar concentrations, ideally. The human (*Homo sapiens*) (**Figure 11A**), rat (*Rattus norvegicus*) (**Figure 11B**), and mouse (*Mus musculus*) (**Figure 11C**) models revealed the inhibitory perspectives of Hesperidin–SPC complex against several targets like hydrolase, enzyme, oxidoreductase, Family A G protein-coupled receptor, transferase, voltage-gated ion channel, primary active transporter, ligand-gated ion channel, etc. The predicted results strongly supported the interactions of lipid complex with multiple targets and have potential to deliver the drug to the action site.

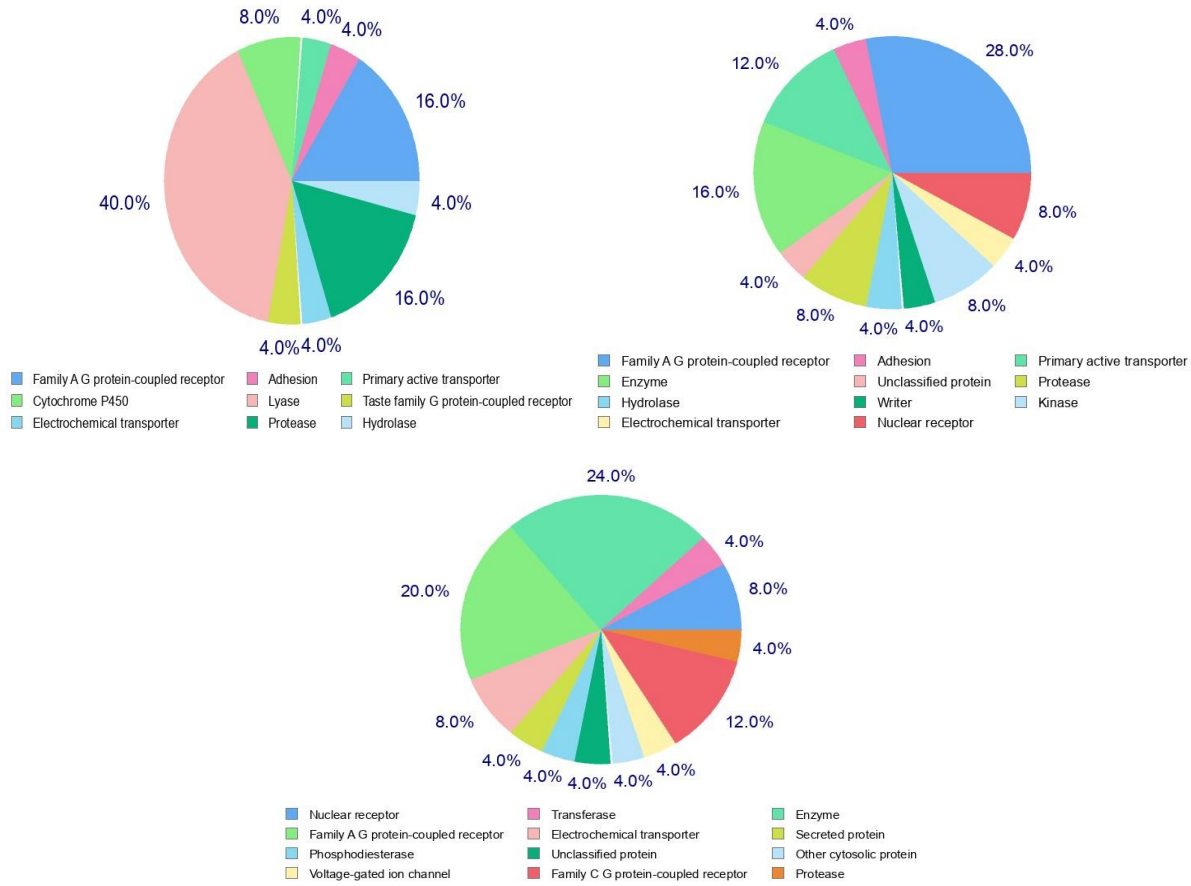

Figure 11. Predicted therapeutic targets of hesperidin-SPC complex against (A) Human, (B) Mouse, and (C) Rat.

4. Conclusion

In conclusion to the above study, the software-assisted statistical optimization of ratio for the formation of hesperidin-SPC complex was successfully performed where critical elements were researched and negative effects of different factors were mitigated. Further, the 1:1 ratio complex was formed and thoroughly characterized by sophisticated analytical instrumentations. The solubility profile revealed the plausible enhancement in solubility of drug after complexation through ampiphilic characteristics. Further, the *in silico* studies on pharmacokinetics and drug targets revealed the therapeutic perspectives of the developed complex against multiple therapeutic targets, allowing for the development of the phytosome precursor natural product-linked lipid complex.

Conflict of interest

Declared none

Funding information

DKM is thankful to Indian Council of Medical Research (ICMR) for providing Senior Research Fellowship (SRF) for the project number 5/3/8/ 25/ITR-F/2019-ITR.

Acknowledgement

The authors acknowledge the Department of Pharmaceutical Sciences for help and support.

5. References

1. Telange DR, Patil AT, Pethe AM, Fegade H, Anand S, Dave VS. Formulation and characterization of an apigenin-phospholipid phytosome (APLC) for improved solubility, in vivo bioavailability, and antioxidant potential. Eur J Pharm Sci 2017;108:36-49.
2. Vu HT, Hook SM, Siqueira SD, Müllertz A, Rades T, McDowell A. Are phytosomes a superior nano delivery system for the antioxidant rutin?. Int J Pharm 2018;548(1):82-91.
3. Babazadeh A, Ghanbarzadeh B, Hamishehkar H. Phosphatidylcholine-rutin complex as a potential nanocarrier for food applications. J Funct Foods 2017;33:134-41.
4. El-Gazayerly ON, Makhlouf AI, Soelm AM, Mohmoud MA. Antioxidant and hepatoprotective effects of silymarin phytosomes compared to milk thistle extract in CCl4 induced hepatotoxicity in rats. J Microencapsul 2014;31(1):23-30.
5. Maryana W, Rachmawati H, Mudhakir D. Formation of Phytosome Containing Silymarin

Using Thin Layer-Hydration Technique Aimed for Oral Delivery. Mater Today Proc 2016;3 (3):855-66.
6. Maryana W, Rahma A, Mudhakir D, Rachmawati H. Phytosome containing silymarin for oral administration: Formulation and physical evaluation. J Biomimet Biomater Biomed Eng 2015;25:54-65.
7. Ripoli M, Angelico R, Sacco P, Ceglie A, Mangia A. Phytoliposome-based silibinin delivery system as a promising strategy to prevent hepatitis C virus infection. J Biomed Nanotechnol 2016;12(4):770-80.
8. Tedesco D, Steidler S, Galletti S, Tameni M, Sonzogni O, Ravarotto L. Efficacy of silymarin-phospholipid complex in reducing the toxicity of aflatoxin B1 in broiler chicks. Poult Sci 2004;83(11):1839-43.
9. Ali SO, Darwish HA, Ismail NA. Curcumin, Silybin Phytosome® and α-R-Lipoic Acid Mitigate Chronic Hepatitis in Rat by Inhibiting Oxidative Stress and Inflammatory Cytokines Production. Basic Clin Pharmacol Toxicol 2016;118(5):369-80.
10. Drobnic F, Riera J, Appendino G, Togni S, Franceschi F, Valle X, Pons A, Tur J. Reduction of delayed onset muscle soreness by a novel curcumin delivery system (Meriva®): a randomised, placebo-controlled trial. J Int Soc Sports Nutr 2014;11(1):31-39.
11. Tung BT, Hai NT, Son PK. Hepatoprotective effect of Phytosome Curcumin against paracetamol-induced liver toxicity in mice. Braz J Pharm Sci 2017;53(1):e16136.
12. Jain PK, Kharya M, Gajbhiye A. Pharmacological evaluation of mangiferin herbosomes for antioxidant and hepato protection potential against ethanol induced hepatic damage. Drug Development and Industrial Pharmacy. 2013;39(11):1840-50.
13. Jain PK, Khurana N, Pounikar Y, Gajbhiye A, Kharya MD. Enhancement of absorption and hepatoprotective potential through soya-phosphatidylcholine-andrographolide vesicular system. Journal of liposome research. 2013;23(2):110-8.
14. Zhang J, Tang Q, Xu X, Li N. Development and evaluation of a novel phytosome-loaded chitosan microsphere system for curcumin delivery. Int J Pharm 2013;448(1):168-74.
15. Hüsch J, Bohnet J, Fricker G, Skarke C, Artaria C, Appendino G, Schubert-Zsilavecz M, Abdel-Tawab M. Enhanced absorption of boswellic acids by a lecithin delivery form (Phytosome®) of Boswellia extract. Fitoterapia 2013;84:89-98.
16. Demir B, Barlas FB, Guler E, Gumus PZ, Can M, Yavuz M, Coskunol H, Timur S. Gold nanoparticle loaded phytosomal systems: synthesis, characterization and in vitro investigations. RSC Adv 2014; 4(65): 34687-95.
17. Naik SR, Panda VS. Hepatoprotective effect of Ginkgoselect Phytosome® in rifampicin induced liver injurym in rats: Evidence of antioxidant activity. Fitoterapia 2008;79 (6): 439-45.
18. Naik SR, Pilgaonkar VW, Panda VS. Neuropharmacological evaluation of Ginkgo biloba phytosomes in rodents. Phytother Res 2006;20(10):901-5.
19. Naik SR, Pilgaonkar VW, Panda VS. Evaluation of antioxidant activity of Ginkgo biloba phytosomes in rat brain. Phytother Res 2006;20(11):1013-6.
20. El-Menshawe SF, Ali AA, Rabeh MA, Khalil NM. Nanosized soy phytosome-based thermogel as topical anti-obesity formulation: an approach for acceptable level of evidence of an effective novel herbal weight loss product. Int J Nanomed 2018;13:307-18.
21. Mishra NK, Joshi KB, Verma S. Inhibition of human and bovine insulin fibril formation by designed peptide conjugates. Mol Pharm. 2013;10(10):3903-12.
22. Deokar SS, Shaikh KS. Exploring Cytotoxic Potential of Ciclopirox on Colorectal Cancer Cells by In-Silico Methodology. Biointerf Res Appl Chem. 2022;12(6):7287-7310.